like transition states, respectively, but the magnitudes and their more quantitative comparison with geometry must await further calculations.

The temperature dependences of these leaving groups do show that for both the SN2 and SN1 reactions the KIE values are inversely proportional to temperature as predicted by simple theory. The experimental results for the two cases reveal that the temperature dependence of the kinetic isotope effects is best evaluated from consideration of the ground-state configuration plus information on the number of isotopically important ground-state vibrational frequencies for a given reactant. The good correlation achieved between the slopes found for the experimental data and the slopes derived from calculated TDF values demonstrates the utility and specificity of the chlorine kinetic isotope effect probe for isotopically important vibrations and the necessity of consideration of the isotopically important ground-state vibrations in deriving models for the transition state from the observed KIE values.

Acknowledgment. This research was supported by the Wisconsin Alumni Research Foundation and the National Science Foundation through Grants GP-8369 and GP-23762.

Beam Maser Measurement of ^{19}F Hyperfine Structure and Relation to Magnetic Shielding in Carbonyl Fluoride

J. H. S. Wang and S. G. Kukolich*

Contribution from the Department of Chemistry, Massachusetts Institute of Technology, Cambridge, Massachusetts 02139.
Received November 15, 1972

Abstract: Hyperfine structure on the $1_{10} \rightarrow 1_{11}$, $2_{11} \rightarrow 2_{12}$, $4_{31} \rightarrow 4_{32}$, and $6_{51} \rightarrow 6_{52}$ rotational transitions in COF_2 was observed with a molecular beam maser spectrometer. The resonance line width (fwhm) ranged from 1.5 kHz on the $1_{11} \rightarrow 1_{10}$ transition to 6 kHz on the highest frequency transitions. The diagonal elements of the spin–rotation tensor obtained are $M_{aa} = -19.77 \pm 0.21$ kHz, $M_{bb} = -13.46 \pm 0.14$ kHz, and $M_{cc} = -7.80 \pm 0.26$ kHz. Magnetic shielding parameters are calculated from experimental results and comparison is made with other molecules.

The dependence of the nuclear magnetic shielding or chemical shift on the molecular structure and chemical properties is very important in nuclear magnetic resonance. Many theoretical calculations[1,2] of the diamagnetic and paramagnetic contributions to the magnetic shielding have been made for small fluorine-containing molecules using either minimal or extended Slater type orbital (STO) basis sets. It is known[1,2] that the diamagnetic contribution, which depends only on the ground electronic state, is insensitive to the choice of basis set. One can calculate the diamagnetic shielding within a few per cent accuracy using a reasonable basis set or the empirical atom dipole model. However, the paramagnetic shielding, which depends on electronic excited states, is very sensitive to the basis wave functions. Unfortunately, there are very few experimental paramagnetic shielding results which can be used to test the choice of basis sets and better understand the relation to the molecular structure. The data most often used in the comparison are the average magnetic shieldings from nmr experiments.

Recently, the magnetic shielding and spin–rotation interaction of fluorine have been studied for a number of small molecules. A direct measurement of the shielding anisotropy for CH_2F_2 was made in the gas phase,[3] and shielding anisotropies for CH_3F, CH_2F_2, and CHF_3[4] were measured in a liquid crystal. An alternative approach to obtain the shielding tensor is to use the measured spin–rotation tensor and calculated values for the diamagnetic shielding. This method was used for CH_3F.[5] In order to better understand the contributions to magnetic shielding and spin–rotation in small molecules, we believe that it is important to have accurate experimental data on spin–rotation and shielding interactions.

Measurements of magnetic hyperfine interactions in a few diatomic molecules, HF,[6] DF,[7] and F_2,[8] were made using molecular beam methods. Some components in the hyperfine structure of COF_2[9] and OF_2[10] were resolved in a microwave spectrometer previously. However, the resolution was not high enough to allow a meaningful comparison with calculations made using different basis sets. In the present experiments, we observe several rotational transitions in COF_2 using a molecular beam maser spectrometer. This system provides improvements in resolution of a factor of 5 to 20 over previous microwave measurements. The high

(1) R. Dichfield, D. P. Miller, and J. P. Pople, *J. Chem. Phys.*, **54**, 4186 (1971).
(2) E. A. Lewis, R. M. Stevens, and W. N. Lipscomb, *J. Amer. Chem. Soc.*, **94**, 4461 (1972).
(3) S. G. Kukolich and A. C. Nelson, *J. Chem. Phys.*, **56**, 4446 (1972).
(4) R. A. Bernheim, D. J. Hoy, T. R. Krugh, and B. J. Lavery, *J. Chem. Phys.*, **50**, 1350 (1969).
(5) S. C. Wofsy, J. S. Muenter, and W. Klemperer, *J. Chem. Phys.*, **55**, 2014 (1971).
(6) M. R. Baker, H. M. Nelson, J. A. Leavitt, and N. F. Ramsey, *Phys. Rev.*, **121**, 807 (1961).
(7) H. M. Nelson, M. R. Baker, J. A. Leavitt, and N. F. Ramsey, *Phys. Rev.*, **122**, 856 (1961).
(8) M. R. Baker, C. H. Anderson, and N. F. Ramsey, *Phys. Rev. A*, **133**, 1533 (1964).
(9) M.-K. Lo, V. W. Weiss, and W. H. Flygare, *J. Chem. Phys.*, **45**, 2439 (1966).
(10) W. H. Flygare, *J. Chem. Phys.*, **42**, 1157 (1965).

resolution allows complete separation of most of the transitions and provides considerable improvement in the accuracy and confidence in hyperfine structure parameters. Also, the signs of the spin–rotation tensor components are clearly determined in this experiment. The accuracy of the spin–rotation tensor components obtained is sufficient to indicate which basis set wave functions are best. Unfortunately calculations are not presently available for COF_2.

The electronic contributions to the spin–rotation and molecular g values both contain matrix elements of angular momentum operator between ground and excited states. We compare the present results with previous Zeeman measurements to obtain $\langle 1/r^3 \rangle$ matrix elements between ground and excited states.

Experimental Section

The molecular beam maser spectrometer has been described before.[11] Briefly, a molecular beam of a sample from a nozzle type source with diameter equal to 0.15 mm passes through an electric quadrupole field which defocusses the lower states in the transition and then passes through a TM_{010} mode cylindrical cavity. A small microwave signal is applied to the cavity in order to stimulate the transition. The observed resonance line width is determined mainly by the transit time of the molecules through the cavity. The line width (fwhm) was about 6 kHz for the 4 in. long cavity used on the $4_{31} \rightarrow 4_{32}$ and $6_{51} \rightarrow 6_{52}$ transitions. The line width was 3 kHz for a 7 in. long cavity used for the $2_{11} \rightarrow 2_{12}$ transition and 1.6 kHz for a 16 in. long cavity used on the $1_{10} \rightarrow 1_{11}$ transition. The microwave signal is phase modulated at 1 kHz and the stimulated emission signal is detected using a superheterodyne receiver and 1 kHz lock-in detector.

Theory of Hyperfine Structure and Analysis of Data

The Hamiltonian describing the spin–spin and spin–rotation interaction for two equivalent nuclei has been described before.[9,12] We review the terms here since there have previously been some errors in applications of the theory. The angular coupling scheme is $I_1 + I_2 = I$, $I + J = F$, where $I_1 = I_2$. The energy due to these interactions is

$$E = C(-1)^{I+J+F}[I(I+1)(2I+1)J(J+1)(2J+1)]^{1/2} \times \begin{Bmatrix} F & I & J \\ 1 & J & I \end{Bmatrix} + D(-1)^{I+J+F}[I(I+1) + 4I_1(I_1+1)] \times \left[\frac{I(I+1)(2I+1)}{(2I-1)(2I+3)}\right]^{1/2} \left[\frac{J(J+1)(2J+1)}{(2J-1)(2J+3)}\right]^{1/2} \begin{Bmatrix} F & I & J \\ 2 & J & I \end{Bmatrix} \quad (1)$$

The spin–rotation constant for a rotational state is defined as $C = \Sigma_g \langle J_g^2 \rangle M_{gg}/J(J+1)$ where $\langle J_g^2 \rangle$ is the square of the rotational angular momentum along three principle inertial axes and M_{gg} are the diagonal elements of the spin–rotation tensor. The strength of the spin–spin interaction D is given by

$$D = \frac{1}{2}\frac{\mu_N^2 g_F^2}{r^3}\left[1 - \frac{3[\langle J_a^2\rangle\alpha^2 + \langle J_b^2\rangle\beta^2 + \langle J_c^2\rangle\gamma^2]}{J(J+1)}\right] \quad (2)$$

where α, β, and γ are the direction cosines of a line between two nuclei along the three principle axes, μ_N is the nuclear magneton, g_F the fluorine g value, and r the fluorine–fluorine internuclear distance. This term can be computed from the geometry. Note that the spin–spin interaction is the extension of Ramsey's formula from a linear molecule to an asymmetric rotor. The formula in ref 9 is only valid when $I_1 = I_2 = 1/2$ as in COF_2, H_2CO, and H_2O. The formula in ref 10 is not suitable for the case $I_1 = I_2 = 1/2$ so the spin–rotation coefficients derived in that paper for H_2CO are not in agreement with our results.

Due to symmetry considerations, only the rotational states with odd K_{-1} values show the hfs splittings in COF_2. The results of the hfs measurements for several transitions are listed in Tables I–IV. Transition components with deviations greater than 1 kHz were unresolved or very weak. The spectrum of the $2_{11} \rightarrow 2_{12}$ transition is illustrated in Figure 1. The hyperfine splitting between two hyperfine components is independent of the center frequency of the rotational transition. One can therefore obtain better information on M_{gg} by fitting these splittings rather than the transition frequencies. Due to the relatively small centrifugal stretching in COF_2, we have not included possible variations of spin–rotation strengths with rotational state. All transitions were fit with the same spin–rotation tensor. The least-squares fit results for the

Table I. Experimental and Calculated Hfs for COF_2 $1_{10} \rightarrow 1_{11}$ Transition[a]

$F' \rightarrow F$	Data	Calcd	Dev
$1 \rightarrow 2$	−28.78	−27.74	−1.04
$0 \rightarrow 1$	−19.23	−19.45	0.13
$2 \rightarrow 2^b$	1.28	1.17	0.11
$1 \rightarrow 0^b$	1.28	2.62	−1.34
$1 \rightarrow 1$	5.09	5.50	−0.41
$2 \rightarrow 1$	35.65	35.40	−0.25

[a] Frequencies of transitions in kHz relative to line center at 5,872,120.19 kHz. [b] Unresolved.

Table II. Experimental and Calculated Hfs for COF_2 $2_{11} \rightarrow 2_{12}$ Transition[a]

$F' \rightarrow F$	Data	Calcd	Dev
$2 \rightarrow 3^b$	−31.73	−30.29	−1.44
$1 \rightarrow 2^b$	−31.73	−32.75	0.92
$1 \rightarrow 1$	−16.12	−16.82	0.70
$2 \rightarrow 2^b$	3.35	5.49	−2.14
$3 \rightarrow 3^b$	3.35	3.28	0.07
$2 \rightarrow 1$	21.60	21.42	0.18
$3 \rightarrow 2$	39.14	39.06	0.08

[a] Frequencies in kHz relative to line center at 17,616,234.96 kHz. [b] Unresolved.

Table III. $4_{31} \rightarrow 4_{22}$ Transition Frequencies Relative to Line Center at 17,404,744.52 kHz

$F' \rightarrow F$	Data	Calcd	Dev
$5 \rightarrow 5^a$	−2.86	−2.94	0.08
$3 \rightarrow 3^a$	−2.86	−2.63	−0.23
$4 \rightarrow 4$	5.81	5.63	0.18

[a] Unresolved.

Table IV. $6_{51} \rightarrow 6_{52}$ Transition Frequencies Relative to Line Center at 17,074,513.64 kHz

$F' \rightarrow F$	Data	Calcd	Dev
$7 \rightarrow 7$	−7.18	−7.45	0.27
$6 \rightarrow 6^a$	5.27	5.64	−0.37
$5 \rightarrow 5^a$	5.27	3.49	1.78

[a] Unresolved.

(11) S. G. Kukolich, *J. Chem. Phys.*, **50**, 3751 (1969).
(12) D. W. Posener, *Aust. J. Phys.*, **11**, 1 (1958).

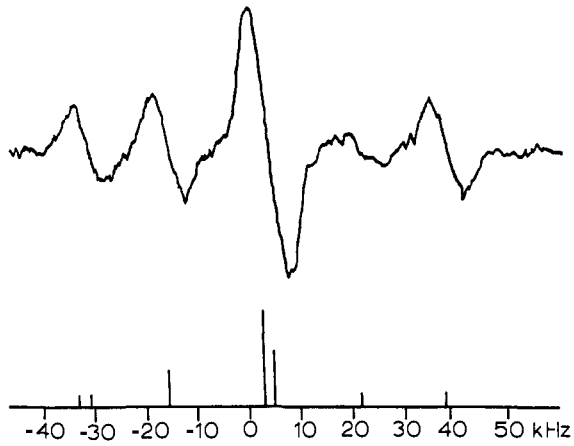

Figure 1. Chart recorder trace of the $2_{11} \rightarrow 2_{12}$ transition in COF_2. The frequency is in kHz relative to the line center at 17,616,235.07 kHz.

diagonal elements in the spin–rotation tensor are shown in Table V. The present results are more accurate,

Table V. Diagonal Elements of Spin–Rotation Tensor and Their Two Contributing Parts (in kHz)[a]

	M_{gg} experimental	M_{gg}(n) nuclear	M_{gg}(e) electronic
M_{aa}	−19.77 ± 0.21	7.68	−27.45
M_{bb}	−13.46 ± 0.14	4.13	−17.59
M_{cc}	−7.80 ± 0.26	5.89	−13.68

[a] Sign has been transformed to the molecular frame scheme.

but essentially in agreement with the earlier work.[9] From these results, one can calculate the center frequency and hfs parameters.

Magnetic Interactions of ^{19}F in COF_2

The spin–rotation tensor is the sum of two components, a term due to the motion of the nuclei and a term from the electrons.[13a] M_{gg}^{k} is defined in eq 3, where

$$M_{gg}^{k} = M_{gg}^{k}(\mathrm{n}) + M_{gg}^{k}(\mathrm{e}) = \frac{2e\mu_n g_k G_{gg}}{\hbar c} \sum_l{}' Z_l r_l^{-3}[r_{lk}^2 - (r_{lk})_g^2] + \frac{2e\mu_n g_k G_{gg}}{\hbar mc} \sum_{p<0} \left[\frac{\langle 0|L_g|p\rangle\langle p|L_g/r^3|0\rangle + \mathrm{cc}}{E_0 - E_p} \right] \quad (3)$$

M_{gg}^{k}(n) can be calculated from the geometry of the molecule. The symbols are defined in ref 13a. The experimental total spin–rotation tensor and the nuclear and the electronic contributions are given in Table V.

It is well known that the nuclear magnetic shielding tensor σ_{xx} can be separated into diamagnetic and paramagnetic terms[14] as

$$\sigma_{xx} = \sigma_{xx}^{\mathrm{d}} + \sigma_{xx}^{\mathrm{p}} \quad (4)$$

Since the electronic contribution to the paramagnetic term has the same form as the electronic contribution to the spin–rotation, we may write the paramagnetic shielding in terms of the spin–rotation tensor as follows.

$$\sigma_{xx}^{\mathrm{p}} = \frac{e^2}{2mc^2}\left\{\frac{M_{xx}I_{xx}c}{e\hbar\mu_N g_I} - \sum_n{}' \frac{Z_n}{r_n^3}(y_n^2 + z_n^2)\right\} = \sigma_{xx}^{\mathrm{sr}} + \sigma_{xx}^{\mathrm{N}} \quad (5)$$

All of the terms have been defined previously.[13a] This expression can be calculated from our spin–rotation tensors. Combining these values with the diamagnetic shielding from the atom dipole model,[13b] one can obtain the magnetic shielding tensors and the average value. All the shielding tensor parameters are listed in Table VI.

Table VI. Elements of Magnetic Shielding Tensors for COF_2[a]

	Diamagnetic contribution[b]	Paramagnetic contribution	Total
σ_{aa}	582.3	−406.0	176.3
σ_{bb}	542.4	−261.5	280.9
σ_{cc}	633.5	−406.7	226.8
σ_{av}	586.1	−358.1	228.0
σ_{exp}			219.0

[a] Units are ppm. Paramagnetic contributions are calculated from measured spin–rotation data. [b] See ref 13b.

We note that if the shielding tensor were cylindrically symmetric about the C–F bond, then $\sigma_{aa} - \sigma_{bb} = (\cos^2\phi - \sin^2\phi)(2\sigma_{cc} - \sigma_{aa} - \sigma_{bb})$, where ϕ is one-half the F–C–F angle. From this relation we calculate $\sigma_{aa} - \sigma_{bb} = -1$ ppm. From the data the value of $\sigma_{aa} - \sigma_{bb} = -105$ ppm, indicating that the shielding is not cylindrically symmetric about the C–F bond direction.

Discussion

In Table VII we obtain the absolute average magnetic shielding value, 226 ± 15 ppm, by combining the spin–rotation tensor and the diamagnetic shielding from the empirical atom dipole model. This value is within the range of the experimental value 219 ppm from nmr experiments.[9] It is known that the absolute shielding value is very difficult to obtain in nmr experiments, especially in the gas phase. If the diamagnetic shielding could be calculated within 1%, we believe that the value obtained by combining it with the paramagnetic part derived from spin–rotation tensors is more reliable than the value measured in the liquid-phase nmr experiments.

Table VII. Magnetic Shielding Parameters of Small Fluorine Compounds[a]

Molecule	σ_{av}	σ_{av}^{p}	σ_{av}^{d}	$\sigma - \sigma^{sr}$	Ref
CH_3F	468	−56 ± 9	523 ± 10	469 ± 10	5
F_2	−233	−763	530	458	5
CH_2F_2	337	−223 ± 15	560	470	*b*
COF_2	219	−358 ± 10	577 ± 10	460 ± 10	*c*

[a] Units are ppm. The absolute shielding scale used below is from D. Hindermann and C. Cornwall, *J. Chem. Phys.*, **48**, 4148 (1968). [b] S. G. Kukolich, J. H. S. Wang, and D. J. Ruben, to be published. [c] This work.

Flygare and Goodisman[15] have proposed a simple

(13) (a) W. H. Flygare, *J. Chem. Phys.*, **41**, 793 (1964); (b) T. D. Gierke, H. C. Tigelaar, and W. H. Flygare, *J. Amer. Chem. Soc.*, **94**, 330 (1972); T. D. Gierke and W. H. Flygare, *ibid.*, **94**, 7277 (1972).

(14) N. F. Ramsey, *Phys. Rev.*, **78**, 699 (1950).

(15) W. H. Flygare and J. Goodisman, *J. Chem. Phys.*, **49**, 3122 (1968).

relationship between the average magnetic shielding in a molecule and free atom as

$$\sigma_{av} - \sigma_{av}^{sr} = \sigma_{av}^{d} + \sigma_{av}^{N} \simeq \sigma_{av}^{d}(\text{free atom}) = \text{constant} \quad (6)$$

In the case of fluorine, σ_{av}^{d}(free atom) = 470 ppm.[5] Several $\sigma_{av} - \sigma_{av}^{sr}$ values for small molecules are also listed in Table VII, which indicates that eq 6 is a very good approximation.

The electronic parts of both the spin–rotational tensor and the molecular g-value tensor depend on the excited states and it is interesting to compare these quantities. The ratio of these two tensor elements is

$$\frac{M_{gg}^{k}(e)}{g_{gg}^{k}(e)} = \frac{2e\mu_N g_k m}{4\pi M_p c} \frac{\sum_{p>0} \frac{\langle 0|L_g^k|p\rangle\langle p|L_g^k/r^3|0\rangle + cc}{E_0 - E_p}}{2\sum_{p>0} \frac{|\langle p|L_g^k|0\rangle|^2}{E_0 - E_p}} = \frac{2e\mu_N g_k m}{4\pi M_p c}\left\langle \frac{1}{r_g^3}\right\rangle_{0,p} \quad \cdots \quad (7)$$

The origin of the molecular g-value tensor[16] can be translated from the center of mass to the k nucleus. After the translation, the g values can be expressed as

$$g_{gg}(k) = g_{gg}^{k}(n) + g_{gg}^{k}(e) = \frac{4\pi G_g M_p}{\hbar m}\left\{ m\sum_l Z_l[r_{lk}^2 - (r_l - r_k)_g(r_l - r_k)_g] + 2\sum_{p>0}\frac{|\langle p|L_g^k|0\rangle|^2}{E_0 - E_p}\right\} \quad (8)$$

where $g_{gg}^{k}(n)$ can be computed from the geometry. The effects of the translation were very small in COF_2 so they are not included in Table VIII. By the combination of the g values[17] and eq 6 and 7, $\langle 1/r_g^3\rangle_{0,p}$ of several molecules has been calculated and listed in Table VIII. Notice that this quantity $\langle 1/r_g^3\rangle_{0,p}$ is almost isotropic along three principle areas in these molecules. It has been pointed out[9] that

$$\langle 1/r_g^3\rangle_{0,p} \cong 0.43 \times 10^{24}\ \text{cm}^{-3}$$

is much smaller than the average over the ground electronic states

$$\langle 1/r_g^3\rangle = 47.3 \times 10^{24}\ \text{cm}^{-3}$$

It could be that the electronic excited states are nearly orthogonal to the ground state or the energy denominator in the perturbation terms reduces the mixing effects.

(16) W. H. Flygare and R. C. Benson, *Mol. Phys.*, **20**, 225 (1971).
(17) P. Thaddeus, L. C. Krisher, and J. H. M. Loubser, *J. Chem. Phys.*, **40**, 257 (1964); K. D. Tucker, C. R. Tomasevich, and P. Thaddeus, *Astrophys. J.*, **169**, 429 (1971).

Table VIII. Electronic Contribution to Spin–Rotation Tensor and Molecular g Values with Origin at the Appropriate Nucleus[a]

	(Axis) g	$[M_{gg}^{e}(k)/g_N G_g] \times 10^6$	$[G_{gg}^{e}(k)/G_g] \times 10^{12}$	$\langle 1/r_g^3\rangle_{0,p} \times 10^{24}$	Ref
COF_2	a	−0.44	−117.1[b]	0.49	
	b	−0.286	−73.8	0.50	This work
	c	−0.446	−191.7	0.30	
H_2O	a	−0.041	−5.5	0.96	
	b	−0.078	−12.1	0.84	11, *c*
	c	−0.117	−17.7	0.86	
H_2CO	a	−0.079	−42.6	0.24	
	b	−0.078	−63.6	0.16	16, 17, *d*
	c	−0.137	−93.1	0.19	

[a] $\langle 1/r^3\rangle$ for the electronic charge distribution is derived from these parameters. All in cgs units. [b] R. Blickensderfer, J. H. S. Wang, and W. H. Flygare, *J. Chem. Phys.*, **51**, 3196 (1969). [c] S. G. Kukolich and D. J. Ruben, *J. Mol. Spectrosc.*, **38**, 130 (1971). [d] H. B. Bluyssen, A. Dymanus, J. Reuss, and J. Verhoeven, *Phys. Lett. A*, **25**, 584 (1967).

Conclusion

Three diagonal ^{19}F spin–rotation tensor elements are obtained in COF_2. The accuracy of the results of this molecular beam measurement is much higher than that of the previous data,[9] so that we are now able to obtain accurate values of $\sigma - \sigma^{sr}$. We note, however, that our spin–rotation tensor is in excellent agreement with the previous tensor.

The paramagnetic shielding tensors were derived from the spin–rotation tensors, which led to determination of the absolute average magnetic shielding. The large paramagnetic shielding σ_{av}^{p} in COF_2 as compared with CH_2F_2 and CH_3F could be attributed to the π-bonding orbitals which overlap with the p_z orbital of fluorine, since there are some low-lying electronic excited states in COF_2. It would be very interesting to calculate the diagonal elements of the tensors for σ^p and σ^d in COF_2 using different basis sets and to compare these with our experimental results. To the best of our knowledge, these calculations are not available at the present time. It would also be interesting to measure the shielding anisotropies directly.

Acknowledgment. We are grateful to the National Science Foundation for supporting this research. The authors thank Dr. Albert Nelson for his help with this project. They also thank Mr. T. D. Gierke and Professor W. H. Flygare for helpful comments and the use of their unpublished results.